



Optimal ^{99m}Tc activity ratio in the single-day stress-rest myocardial perfusion imaging protocol: A multi-SPECT phantom study

Orazio Zoccarato, PhD,^a Roberta Matheoud, PhD,^c Michela Lecchi, PhD,^d
Camilla Scabbio, PhD,^d Marcassa Claudio, MD,^b and Marco Brambilla, PhD^c

^a Department of Nuclear Medicine, S. Maugeri Foundation, IRCCS, Scientific Institute of Veruno (NO), Veruno, Italy

^b Department of Cardiology, S. Maugeri Foundation, IRCCS, Scientific Institute of Veruno (NO), Veruno, Italy

^c Department of Medical Physics, University Hospital 'Maggiore della Carità', Novara, Italy

^d Health Physics Unit, ASST Santi Paolo e Carlo, Milan, Italy

Received May 18, 2020; accepted Jul 9, 2020

doi:10.1007/s12350-020-02290-2

Background. This investigation used image data generated by an anthropomorphic phantom to determine the minimal ^{99m}Tc rest-stress activity concentration ratio (R) able to minimize the ghosting effect in the single-day stress-first myocardial perfusion imaging, using different positions of the perfusion defect (PD), scanners and reconstruction protocols.

Methods. A cardiac phantom with a simulated PD was imaged under different R using different gamma cameras and reconstruction algorithms. The residual activity from precedent stress administration was simulated by modeling effective half-times in each compartment of the phantom and assuming a delay of 3 hours between the stress and rest studies. The net contrast (NC) of the PD in the rest study was assessed for different R , PD positions and scanner/software combinations. The optimal R will be the one that minimize the NC in the rest images

Results. The activity concentration ratio R , the position of the PD and the scanner/software combinations were all main effects with a statistically significant impact on the NC, in decreasing order of relevance. The NC diminished significantly only for R values up to 2. No further improvement was observed for NC for R values above 2 and up to 3. NC was significantly higher in anteroseptal than in posterolateral positions of the PD and higher for solid-state cameras.

Conclusions. A rest-stress activity concentration ratio R of 2 in single-day stress-first myocardial perfusion imaging is enough to achieve the maximum net contrast in the PD. This ratio should be used to optimize patient's radiation exposure. (J Nucl Cardiol 2021;28:338–49.)

Key Words: Myocardial perfusion imaging; SPECT • patient radiation dose • single-day protocol • stress-first protocol

Electronic supplementary material The online version of this article (<https://doi.org/10.1007/s12350-020-02290-2>) contains supplementary material, which is available to authorized users.

The authors of this article have provided a PowerPoint file, available for download at SpringerLink, which summarises the contents of the paper and is free for re-use at meetings and presentations. Search for the article DOI on SpringerLink.com.

Reprint requests: Marco Brambilla, PhD, Department of Medical Physics, University Hospital 'Maggiore della Carità', Novara, Italy; marco.brambilla@maggioreosp.novara.it

1071-3581/\$34.00

Copyright © 2020 American Society of Nuclear Cardiology.

Abbreviations

AC	Activity concentration
FBP	Filtered back projection
CZT	Cadmium-zinc-telluride
LV	Left ventricle
MPI	Myocardial perfusion imaging
NC	Net contrast
PD	Perfusion defect
R	Rest-stress activity concentration ratio
ROI	Region of interest
WBR	Wide beam reconstruction

See related editorial, pp. 350–353

INTRODUCTION

In diagnostic Nuclear Medicine imaging the amount of the administered radiopharmaceutical activity is always a compromise between image quality and radiation exposure of both patients and staff. Furthermore, in myocardial perfusion imaging (MPI), additional parameters should be accounted for: the choice of the ^{99m}Tc labeled compound and the acquisition protocol, whether single or two-day scheme, the type of gamma camera employed, dedicated to MPI or traditional, the reconstruction algorithm and the patient's habitus.

The single-day protocol has some advantages compared to the dual-day procedure. Above all, it allows for a complete myocardial stress-rest perfusion study in a few hours, thus reducing patient discomfort. The major drawback is related to the residual stress activity which is still present in the myocardial left ventricle (LV) wall when the activity for the rest study must be injected. For instance, in an ischemic patient with an abnormal stress perfusion and an entirely normal rest perfusion, the stress defect may be partially apparent in the rest scan leading to the underestimation of ischemia.¹ To reduce this unwanted contribution (ghosting effect) a multiple of the original stress activity must be injected.

Several rest-stress activity ratios (R) were used in the single-day MPI scheme, ranging from 2 to 4^{2,3} and a consensus of the published procedural guidelines was reached on a 3 ratio for a 2-3-hour delay between the initial stress scan and the subsequent rest scan. In particular, the American Society of Nuclear Cardiology-ASNC recommends to administer three times the stress activity for the rest study with a 2 hours delay between the stress and rest acquisition or a 3.5 to 4:1 ratio of activities with no delay, with a range of activities able to manage patients up to a BMI $\geq 35 \text{ kg/m}^2$ (from 296-444 MBq to 888-1332 MBq for a 70 kg patient imaged in a Anger camera).⁴ Similar ratios are also suggested for other camera/reconstruction algorithms combination.

The first guideline of the European Association of Nuclear Medicine-EANM for perfusion imaging in nuclear cardiology⁵ recommended a ^{99m}Tc activity of 400-500 MBq for the first injection of the single-day imaging protocol and three times more for the second injection with a 3-hour delay between the stress and rest acquisition, based on a prevalent consensus, general experience on myocardial perfusion SPECT and on phantom experiments.⁶

The revised 2015 EANM guidelines for SPECT and SPECT/TC myocardial imaging reported 4 MBq/kg for the first study (250-400 MBq) and 12 MBq/kg (750-1200 MBq) for the second activity injection, confirming the criteria of 3:1 for the activity ratio between the second and first study for the single-day imaging protocol.⁷

The last 2019 EANM guidelines recommend that, when a dedicated cardiac camera is used, the injected ^{99m}Tc activity should be in the range 2.5-3.5 MBq/kg (minimal and maximal activity of 150 MBq and 300 MBq, respectively) for the first injection and, for the second acquisition, in the range 7.5-10.5 MBq/kg (maximal activity of 900 MBq).⁸

Regardless of the absolute values of activity to be injected suggested by the various guidelines, a concern still remains on the dosimetric issue: the 3:1 activity ratio is unfavorable from the patient's radiation protection point of view, compared to the separate-day protocol. Moreover, the rest-stress 3:1 ratio, although suggested and commonly adopted worldwide, does not seem to be supported by a rigorous experimental validation and evidence is limited.

All these factors suggest the need to verify whether the 3:1 activity ratio is mandatory, or, with a different perspective, which could be the minimal rest-stress activity ratio required to minimize the occurrence of crosstalk of stress perfusion defects leading to underestimation of ischemia or overestimation of scar.

Aim of the present study was to experimentally determine in an anthropomorphic phantom the minimal ^{99m}Tc activity ratio able to minimize the ghosting effect in the single-day stress-rest MPI protocol with a 3-hour delay between the stress and rest acquisitions, using different positions of the perfusion defect (PD), scanners and reconstruction protocols.

MATERIALS AND METHODS

Experimental Model

In the single-day stress-rest protocol for the MPI studies the major limitation lays in the identification of the minimum ^{99m}Tc activity to administer in the rest study capable to

minimize the residual image of an ischemic territory possibly still present.

To obtain reliable results, the extreme case of an ideal ischemic territory was hypothesized: a territory that in the stress had no uptake (100% ischemic), while showing in the rest study an uptake exactly equivalent to that of the normal LV walls. Although this is a totally non-physiologic assumption, nevertheless because we evaluated the effect of the stress defect contributing to the subsequent rest scan (“ghosting”), this should be intended as “worst case scenario” and should more than account for less severe ischemic defects.

A 3-hour delay was imposed between the initial stress scan and the subsequent rest scan. This waiting time was selected in order to decrease on-board stress activity and minimize the “ghosting” effect in subsequent resting scan.

Using an anthropomorphic phantom already considered in previous publications,^{9–11} a stress PD was simulated in different myocardial territories and acquired with a Cadmium-Zinc-Telluride (CZT)-based camera and a conventional gamma camera, with the filter-back projection (FBP) algorithm or an iterative algorithm with resolution recovery.

Under these hypotheses, the following three conditions were realized:

- Stress study: the normal LV wall, the LV myocardial cavity, the liver and the mediastinum have the tracer concentration typical of the stress studies.⁹ On the contrary, the simulated lesion does not show any uptake.
- Rest study: all the compartments with the exception of the ischemic territory, have the concentration equal to the residual stress activity linked to the effective half-life of that specific territory¹² plus the activity resulting from the rest study injection. The ischemic territory has a concentration of activity linked only to the contribution of the injected rest activity.
- Blank study: No PD was inserted in the LV wall and the anthropomorphic phantom was prepared by filling each compartment with the same activity concentrations of the stress study.

Gamma Cameras

Two gamma cameras were employed: the Infinia (General Electric) and the Discovery NM 530c with Alcyone technology (General Electric), installed in the same Nuclear Medicine Department (Veruno). The gamma cameras characteristics and the manufacturers’ recommended acquisition and reconstruction protocols are detailed in Table 1. With the Infinia camera two reconstruction protocols were used, the Filtered Back Projection and the Wide Beam Reconstruction (WBR) (UltraSPECT, Haifa, Israel). Overall, three scanner/software combinations were assessed.

Anthropomorphic Phantom

An anthropomorphic phantom of the chest, with inserts simulating lungs, liver, LV wall, LV inner chamber and PD was used (Torso Phantom™ and Cardiac Insert™, Data

Spectrum Corporation, Hillsborough, NC, USA). The PD insert (45° x 2 cm, volume = 3.8 mL) can simulate a transmural fixed/reversible PD, when filled with non-radioactive/radioactive water, respectively. The lung inserts, filled with Styrofoam™ beads and non-radioactive water, were used to simulate lung tissue attenuation density. The other phantom compartments were filled with ^{99m}Tc-solutions of different activity concentrations (AC) in MBq/mL, fixed by the experimenter and detailed below.

For all preparations, the ^{99m}Tc activity was measured by using the same dose calibrator (AtomLab 100 plus, Biodex) which underwent a routine quality control program including accuracy and constancy tests that always showed values within the limits of 5%. For each session, the preparation of each ^{99m}Tc activity used to fill the compartments of the anthropomorphic phantom was obtained by volume dilution using calibrated pipettes.

Session 1: Stress Study

A fixed transmural defect was simulated by placing the PD insert filled with non-radioactive water in the LV wall. The other phantom compartments were filled with the ^{99m}Tc solution concentrations reported in Table 2.

The loading contrast of the PD with respect to the LV wall (LC_{PD}) is defined as:

$$LC_{PD}(\%) = \frac{AC_{LV} - AC_{PD}}{AC_{LV} + AC_{PD}} * 100, \quad (1)$$

where AC_{LV} and AC_{PD} are the ^{99m}Tc solution concentration in MBq/mL in the LV wall and PD according to Tables 2 and 3. The LC_{PD} are derived from the loading scheme of the phantom and are not measured on images. Therefore, they are fixed by the experimenter and expressed as a ratio of AC values. In the stress study experiment LC_{PD} is 100%.

For each setup, the cardiac insert was positioned such that the PD was in the anterior, lateral, posterior and septal walls. The whole procedure was repeated twice sequentially on each camera and overall 16 acquisitions were performed (1 phantom realization x 2 gamma cameras x 4 PD positions x 2 acquisitions). For each acquisition a total of 3 and 1.6 Mc were collected, on Infinia and Discovery NM 530c gamma cameras respectively, according to the manufacturers’ recommendations. Finally, each acquisition was reconstructed by using the parameters reported in Table 1 for the correspondent gamma camera, obtaining the transaxial slices.

Session 2: Rest Study

To simulate the rest condition in a single-day protocol, one should first consider the residual ^{99m}Tc activity in each compartment of the anthropomorphic phantom, due to the previous stress study, at the time of the rest activity administration which was set 3 hours late.¹³ The residual activities can be obtained by decay correcting those used in the stress phantom preparation (Table 2) for the associated effective

Table 1. Acquisition and reconstruction parameters for the gamma cameras used in this study.

Gamma camera	Discovery NM 530c	Infinia	
Type of Crystal	CZT	NaI(Tl)	
Collimator	Multi-pinhole	Low energy parallel hole	
Acquisition parameters			
Number of projections	19	60	
Angular range	180°	180°	
Voxel size (mm × mm)	4 × 4	6.6 × 6.6	
Total counts collected	1.6 Mc (stress&rest)	4Mc (rest) - 3Mc (stress)	
Reconstruction parameters			
Reconstruction algorithm (iteration & subsets)	Iterative 3D 60 × 1	FBP Butterworth (order 10, cutoff .4 cm ⁻¹)	WBR As defined by the manufacturer (Xpress3 setup)
Post reconstruction filter	Butterworth (order 7, cutoff .37 cm ⁻¹)	-	-
Resolution correction	-	-	3D modeling of the PSF in the system matrix
Noise regularization	Green One-Step-Late (OSL) correction with $\alpha = .5 \div \beta = .4$	-	STANDARD strength (ST)
Slice thickness, mm	4.0	6.6	6.6

Table 2. Details of the compartments of the anthropomorphic phantom, activity and activity concentrations used in the stress study experiment

Compartment	Volume (mL)	Activity (MBq)	Activity concentration (MBq/mL)	Activity concentration ratio with respect to chest
LV wall	121.43	20.4	.168	20.4
Inner chamber	63.89	.5	.008	1.0
Perfusion defect, PD	3.8	0	0	0
Liver	1166	117.6	.101	12.2
Chest	9704	80	.008	-

half-lives¹²; these values are reported in the third column of Table 3.

Thus, the total ^{99m}Tc activity present in each compartment ‘i’ (with the exception of the PD) will be the sum of the residual stress activity plus the rest activity that is equivalent to R times (R = 1.0, 1.5, 2.0, 2.5 and 3.0) that of the stress study:

$$\text{Total rest activity (i)} = \text{Residual stress activity (i)} + R \times \text{initial stress activity (i)}. \quad (2)$$

For the PD which had no activity in the stress study the total rest activity will be the same as that of the LV wall had in the stress study multiplied by the ratio factor ‘R’:

$$\text{Total rest activity(PD)} = R \times \text{initial stress activity (LV)}. \quad (3)$$

The LC_{PD} values in the rest experiment were: 24.2%, 17.5%, 13.8%, 11.3%, and 9.6% for R = 1.0, 1.5, 2.0, 2.5 and 3.0, respectively (Figure 1). In this simple pathophysiological model of the left ventricle, LC_{PD} represents the real contrast between the healthy and diseased tissue of the patient’s LV walls. It is a value connected but different from the contrast value that we evaluate with our acquisition/reconstruction systems.

However, LC_{PD} draws our attention to two simple evidences:

Table 3. Residual activity from precedent stress ^{99m}Tc administration and total activity deriving from additional rest administration, for each compartment in the anthropomorphic phantom

Compartment	Effective half-life (minutes)	Residual ^{99m} Tc stress activity (MBq)	Total rest ^{99m} Tc activity (Residual + R × stress activity) (MBq)				
			R = 1.0	R = 1.5	R = 2.0	R = 2.5	R = 3.0
Normal myocardium (LV wall)	278	13.0	33.4	43.6	53.8	64.0	74.2
Inner chamber	278	.3	.9	1.1	1.4	1.6	1.9
Ischemic myocardium (PD)	224	.0	.6	1.0	1.3	1.6	1.9
Liver	67	18.3	135.9	194.7	253.5	312.3	371.1
Chest	278	51.1	131.1	171.1	211.1	251.1	291.1

- a. it decreases as R increases, but
- b. for a fixed R, it increases as the time interval between stress and rest decreases, rising so the risk of underestimating ischemia or overestimating the scar.

In the 5 rest experiments with different Rs, the PD positioning and the anthropomorphic phantom acquisition steps were performed exactly following the description reported in Session 1. Overall, 80 acquisitions were performed (5 phantom realization × 2 gamma cameras × 4 PD positions × 2 acquisitions). For each acquisition a total of 4 and 1.6 Mc were collected, on Infinia and Discovery NM 530c gamma cameras respectively, accordingly to the manufacturers’ recommendations. Finally, each acquisition was reconstructed by using the parameters reported in Table 1 for the correspondent gamma camera, obtaining transaxial slices.

Session 3: Blank Study

No PD was inserted in the LV wall and the anthropomorphic phantom was prepared by filling each compartment with the activity concentrations reported in Table 2; Four and 6 phantom realizations were performed for Discovery 530c and Infinia gamma cameras, respectively. Each realization was acquired twice with a complete phantom repositioning, then the transaxial slices were reconstructed accordingly to parameters reported in Table 1.

Notwithstanding a homogeneous distribution of the activity concentration in the phantom’s LV compartment, the transaxial images of the LV did not exhibit uniform counts per pixels, due to the camera characteristics and a well-known self-attenuation artifact, as already shown by other authors.¹⁴ The combination of these effects can be appreciated in Figure 2. Since we are interested in assessing the contrast between the LV wall and the PD, positioned in different regions of the same LV wall, it is first necessary to clear the measured image contrast between the LV and the PD from this “blank”

contrast which is specific for each scanner/software combination and this can be done by simple subtraction.

Image Analysis

The transaxial slices reconstructed in each session, were then realigned according to cardiac orientation to obtain short axis slices. This choice was driven by the consideration that polar plots used in clinical evaluation are derived from the short axis slices.

For Sessions 1 and 2, the image contrast of the PD with respect to the LV wall (IC_{PD}) was evaluated by drawing regions of interest (ROI) on the short axis slices that best intercepted the PD:

$$IC_{PD} = \frac{\langle C_{LV} \rangle - \langle C_{PD} \rangle}{\langle C_{LV} \rangle + \langle C_{PD} \rangle} * 100, \tag{4}$$

where C_{LV} is the average counts per pixel in the LV ROI, C_{PD} is the average counts per pixel in the PD ROI

For each gamma camera and for each position of the PD, two ROIs were defined, one for the LV wall and the other for the PD (Figure 3). Each set of ROIs was used in C_{PD} evaluation, with minor adjustments between the repeated acquisitions.

From realizations of Session 3, the contrast of the LV wall of the blank phantom was evaluated on the correspondent short axis slices, by using the same ROIs in the same positions defined in the previous step:

$$BC_{PD} = \frac{\langle C_{LV} \rangle - \langle C_{PD} \rangle}{\langle C_{LV} \rangle + \langle C_{PD} \rangle} * 100. \tag{5}$$

For each gamma camera, the BC_{PD} value was evaluated for each position of the PD by averaging the correspondent values obtained in each realization/reconstruction.

Finally, for Sessions 1 and 2, for each gamma camera and each PD position the net contrast (NC) was defined as:

Sessions 1 & 2 – PD and LV-wall loading scheme

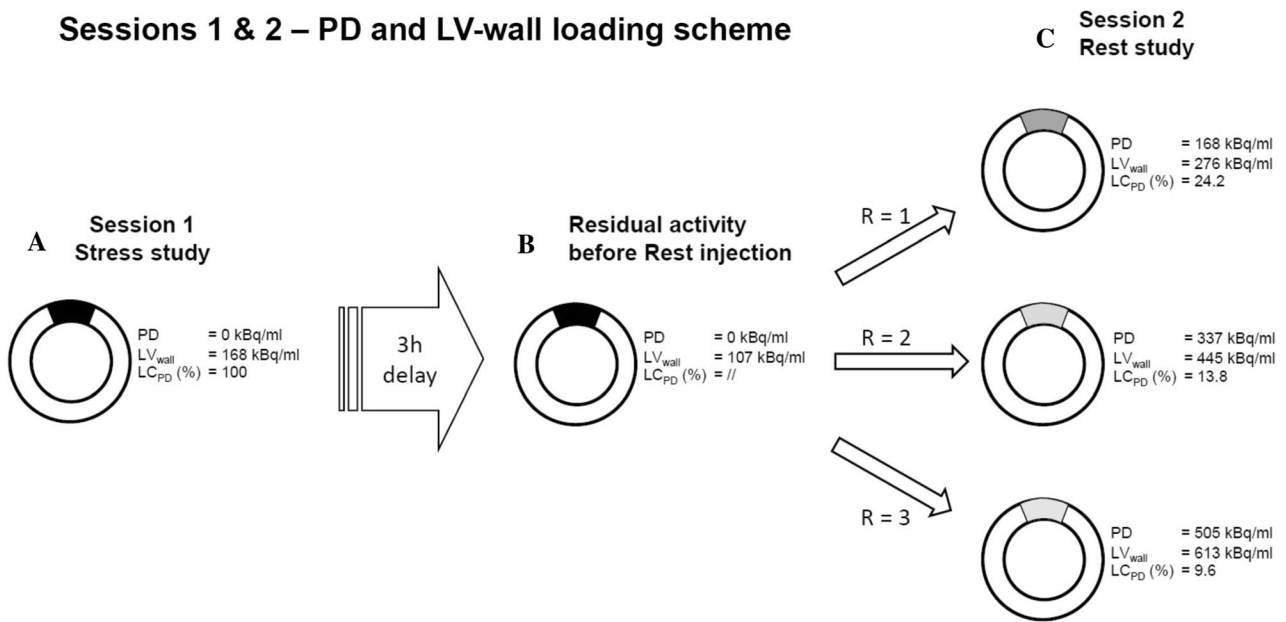


Figure 1. Phantom loading scheme (in kBq/mL) for the PD and the LV wall. **A** Session 1—Stress Study—the PD was filled with non-radioactive water. **B** According to the effective half-life, the 3 hours residual activity concentration is shown. **C** Session 2—rest studies—the resulting activities concentrations (residual + rest injection) employed for the rest studies are shown in case of $R = 1$, 2 or 3 respectively. The corresponding LC_{PD} are also showed. The activities used for the other phantom compartments and the preparations at intermediate concentrations ($R = 1.5$ and $R = 2.5$ not shown here) were carried out in a similar way using the values reported in Table 3.

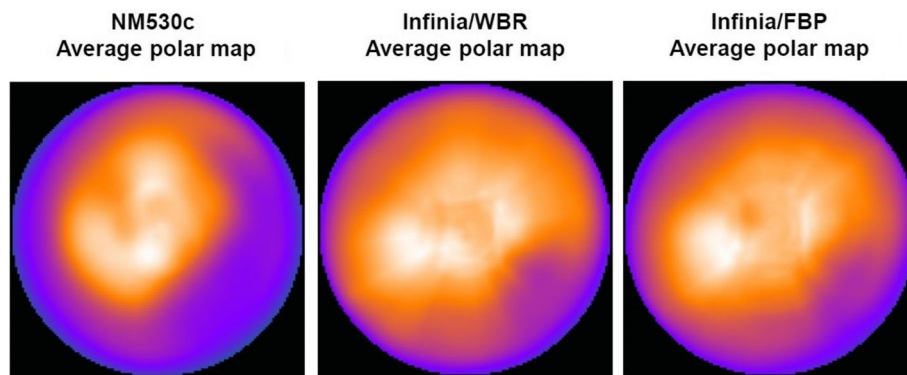


Figure 2. Average polar map images obtained with the blank phantom and imaged with the three scanner/software combinations.

$$NC = IC_{PD} - BC_{PD} \tag{6}$$

The NC values obtained in Session 1 (NC_0) were used as reference values of maximum net contrast for each gamma camera and PD position.

The NC values obtained in Session 2 for all phantom realizations ($R = 1.0, 1.5, 2.0, 2.5$ and 3.0) were used in subsequent analyses.

From all the above, it follows that the optimal R will be the one that minimize the NC in the rest images or, to say it in other words, the criteria for optimality is to find the minimum R where no statistically significant differences are observed in the mean NC corresponding to this R and the mean NC measured at the next increasing value of R .

Statistical Analysis

The impact of the different *R*s, scanner/software combinations and position of the PD on NC, was assessed by a three-way main effect ANOVA. *R*, the position of the PD and the scanner/software combinations were considered as independent variables (factors) and NC as the dependent variable.

A post hoc test (Scheffé *F* test) was performed to identify the main sources of variability. If a significant *F* value was found for one independent variable, then this was referred as a main effect. When a main effect was found, a post hoc test (Scheffé test) was performed to compare the dependent variable upon the levels of the factor 2×2 , thus identifying the main sources of variability.

Analysis was performed with Statistica version 6.0 (StatSoft Inc., Tulsa, OK, USA) using a two-sided type I error rate of $P = .05$.

RESULTS

Figure 4 shows the stress and rest short axis slices with the PD at increasing *R* obtained with the WBR scanner.

The behavior of NC as a function of the activity concentration ratio *R*, the position of the PD and the scanner/software combinations is shown in Figures 5, 6 and 7, respectively. Table 4 shows NC values for Session 1 and 2 for each scanner/software combination and for each position of the PD, while Table 5 reports NC values for each scanner/software combination for the different *R* values.

The activity concentration ratio *R* ($F = 105$; $P < .0001$), the position of the PD ($F = 23$; $P < .001$)

and the scanner/software combinations ($F = 19$; $P < .001$) were all main effects with a statistically significant impact on the NC, in decreasing order of relevance.

Post hoc test of the different *R* showed a significant decrease in NC values from 1 to 1.5 (17.2 ± 5.0 vs 11.3 ± 4.1 ; $P < .0001$) from 1.5 to 2 (11.3 ± 4.1 vs 8.3 ± 2.6 ; $P < .0001$); no significant differences were found between 2 and 2.5 (8.3 ± 2.6 vs 7.8 ± 3.4 ; $P = .94$) and 2.5 and 3 (7.8 ± 3.4 vs 7.3 ± 2.7 ; $P = .95$) (Figure 5).

Post hoc test of the different position of the PD did not show any significant difference in NC between the anterior and septal positions (12.4 ± 4.9 vs 11.2 ± 6.3 ; $P = .18$) or between the lateral and posterior position (9.8 ± 4.1 vs 8.5 ± 4.6 ; $P = .11$). On the contrary, a significant difference was found between the septal and lateral positions (11.2 ± 6.3 vs 9.8 ± 4.1 ; $P = .047$) (Figure 6)

Post hoc test of the different scanner/software combinations showed a significant decrease in NC from the CZT scanner to the Infinia/WBR (11.8 ± 5.8 vs 9.4 ± 4.7 ; $P < .001$), while no significant differences were found between from Infinia/WBR to Infinia/FBP (9.8 ± 4.6 ; $P = .69$) (Figure 7). This behavior was mainly due to the higher NC values shown by the CZT scanner in the posterior position ($11.1 \pm .5$) when compared to the corresponding values of the Infinia/WBR ($7.2 \pm .5$) or the Infinia/FBP ($6.7 \pm .6$).

DISCUSSION

In the last decade, many efforts have been made to reduce the patients' dose in myocardial perfusion studies. Following the ASNC guidelines, the range of total radiation exposure of a 70 kg patient undergoing a stress/rest ^{99m}Tc perfusion study is now 9-13.5 mSv with an Anger camera and a ratio of rest to stress activity of 3:1.⁵ The technical advancements of solid-state SPECT cameras has been used to reduce patient's radiation exposure up to 50% while preserving diagnostic accuracy,¹⁵ regional perfusion defect size and functional parameters¹⁶ The lowest total radiation exposure with current SPECT MPI (1 mSv) can be accomplished clinically by performing stress-only imaging with a solid-state camera system.¹⁷ Noteworthy, since each gamma camera has specific design and features for image acquisition and analysis, the last EANM guidelines have been separated into three different sections, one for each cardiac-centered camera commercially available.⁷

The results of the present study referred to a stress followed by rest imaging procedure (stress-first protocol), which is advantageous in term of patient doses

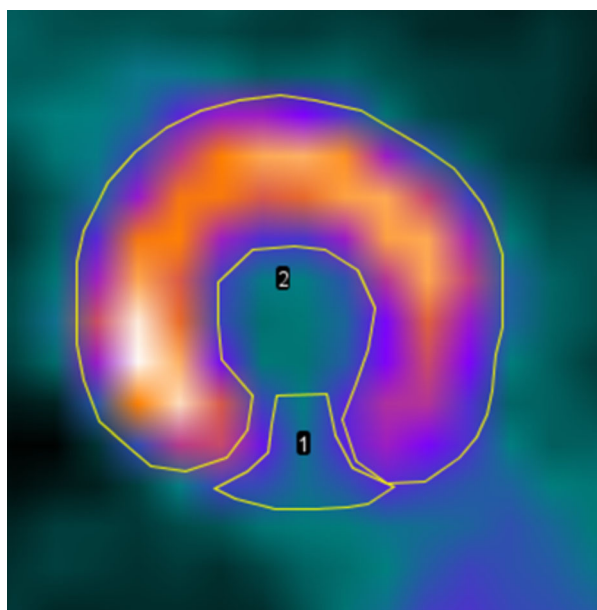


Figure 3. ROIs on PD and LV wall drawn on short axis slice intercepting the PD. 1: LV wall; 2: PD.

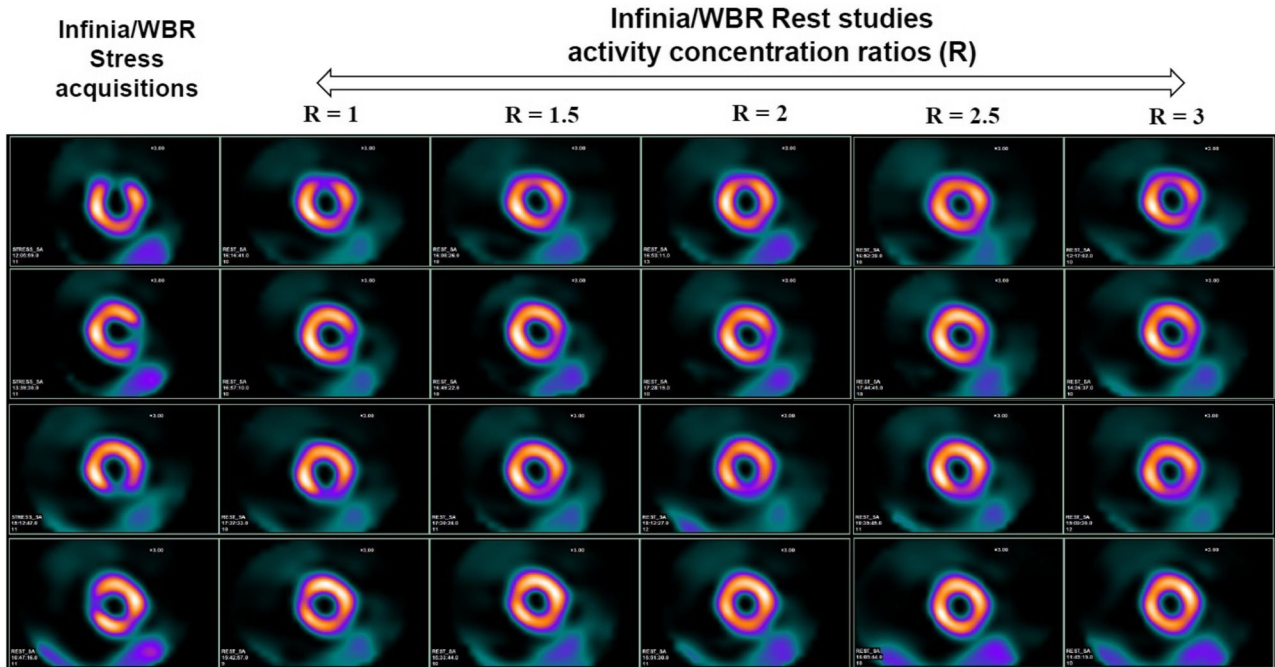


Figure 4. Stress and Rest best short axis slices with the PD at increasing R values obtained with the Infinia/WBR scanner. From first to last row the PD located in mid anterior, lateral, posterior and septal LV wall, respectively. The first column shows the best stress short axis slices. From the second to the sixth column, the same best short axis slices obtained with increasing R s are displayed.

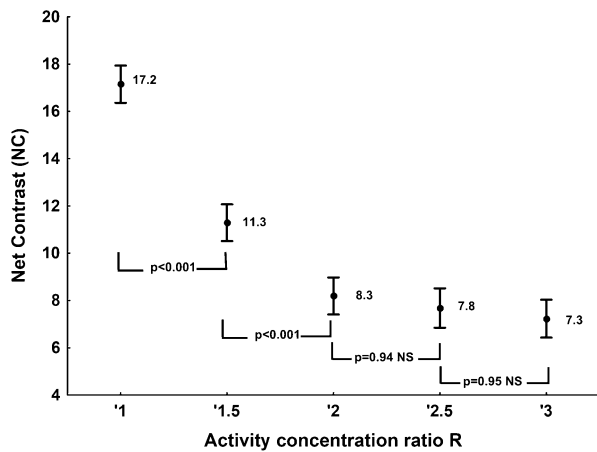


Figure 5. NC as a function of R . Points represent least square averages; vertical bars represent 95% confidence intervals for the mean values.

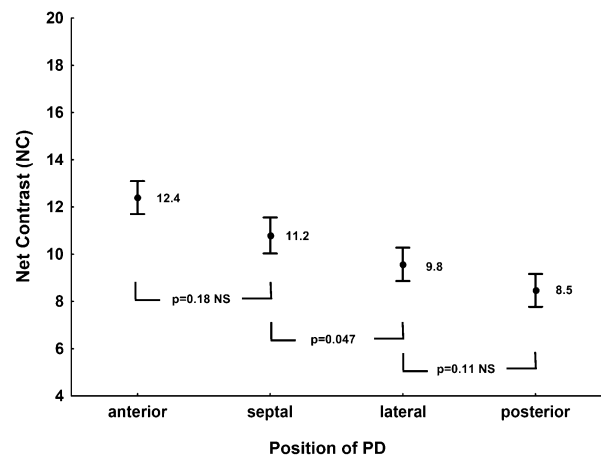


Figure 6. NC as a function of the position of the PD. Points represent least square averages; vertical bars represent 95% confidence intervals for the mean values.

since, in the case of normal stress study (normal perfusion, volumetric, kinetics and function), the study at rest can be avoided (stress-only protocol).¹⁸⁻²⁰ The stress-first protocol further reduces the effective dose to the patients when X-ray computed tomography scanning is performed for attenuation correction.²¹

The total radiation exposure for a patient undergoing a single-day stress/rest perfusion study is about 100% higher than that of a 2-day protocol. Thus, the single-day protocol is unfavorable from the patient's radiation protection point of view if compared to the corresponding separate-day protocol. In parallel the single-day imaging protocol causes an increase in staff

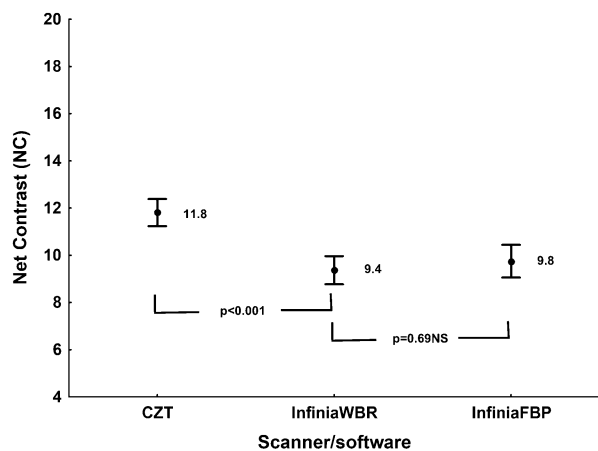


Figure 7. NC as a function of the scanner/software combination. Points represent least square averages; vertical bars represent 95% confidence intervals for the mean values.

doses, albeit to a lesser extent, mainly in the busy nuclear medicine departments.

In this context, the aim of the present study was to determine the optimal R needed to minimize the NC in the rest image, which can be seen as an index of persistence of the ghost stress image on the subsequent rest image and considering three different scanner/software combinations: Discovery NM 530c, Infinia with FBP or WBR algorithms.

Independently on the scanner/software combinations, the results showed that ratios of rest to stress activities greater than 2:1 did not provide a statistically significant improvement in term of perfusion defect contrast with respect to the LV wall. Thus, for the rest study, an injection of two times the stress activity seems enough to reduce the ghost effect after 3-hour delay between the two scans. A ratio of 2:1 would allow a

Table 4. NC values obtained in session 1 (stress study, cold defect) and 2 (rest study) reported for each scanner/software combination and position of the PD

Session	Scanner/software combination	Lesion position				Mean + sd
		anterior	septal	lateral	posterior	
1	Discovery NM 530c	56.1 ± 2.4	47.5 ± 3.0	35.3 ± 2.8	32.8 ± 2.1	42.9 + 9.9
	InfiniaWBR	43.4 ± 10.3	30.6 ± 5.7	29.4 ± 9.2	35.6 ± 5.1	34.7 + 8.5
	InfiniaFBP	45.4 ± 2.8	33.6 ± 5.8	34.0 ± 4.4	25.6 ± 3.8	35.1 + 9.4
	Mean + sd	48.5 + 8.4	38.7 + 9.1	32.8 + 6.5	31.7 + 5.5	
2	Discovery NM 530c	12.8 + 4.6	13.0 + 7.7	10.2 + 5.3	11.2 + 4.7	11,8 + 5.8
	InfiniaWBR	10.9 + 5.6	11.6 + 4.6	8.8 + 2.8	7.2 + 4.5	9.5 + 4.7
	InfiniaFBP	13.5 + 3.9	8.2 + 4.5	10.4 + 3.6	6.7 + 2.8	9.8 + 4.5
	Mean + sd	12.3 + 4.9	11.3 + 4.6	9.7 + 4.1	8.5 + 4.6	

Data for each scanner/software combination in session 2 are averages of the net contrast values for the five different Rs

Table 5. NC values obtained in Session 2 (rest study) reported for each Scanner/software combination and R

Scanner/software combination	Activity concentration ratio R				
	1	1.5	2	2.5	3
Discovery NM 530c	20.4 + 4.5	14.6 + 2.3	8.5 + 1.6	7.7 + 2.1	7.9 + 2.9
InfiniaWBR	14.8 + 4.7	9.8 + 4.2	8.1 + 2.3	8.0 + 4.5	6.1 + 2.3
InfiniaFBP	16.0 + 4.0	8.8 + 3.0	8.3 + 3.7	8.2 + 3.6	8.1 + 2.5
Mean ± sd	17.2 + 5.0	11.3 + 4.1	8.3 + 2.5	7.8 + 3.4	7.3 + 2.7

further 25% reduction in patients' dose in case of the single-day protocol.

The reliability of the results provided in this study resides in the extreme model of ischemic tissue that was simulated and in the evaluation of NC on a static phantom. Indeed, it would be unlikely to be faced, *in vivo*, with ischemic territories showing such extreme behaviors, but even if it were so, it should be considered the further reduction in the measured contrast values due to the movement of the left ventricle. Therefore, based on these considerations, we believe that the results provided in this phantom model should be quite robust with respect to an *in vivo* validation.

Moreover, our findings confirm and extend to different gamma camera models and different position of the simulated PD the results reported by van Dijk et al. in a patient study using a single SPECT camera based on CZT and Alcyone technology (GE Healthcare) and with fixed positions of the perfusion defects in the phantom experiment.¹³

The position of the PD was the second main effect in order or relevance with a statistically significant impact on the NC. While there were no significant differences in NC between the anterior and the septal and between the lateral and posterior myocardial regions, a significant difference was present in NC between the anteroseptal and posterolateral territories, which is agreement with the different characteristics of attenuation experimented by those two myocardial regions. Since NC can be interpreted as an index of persistence of the ghost stress image on the subsequent rest image, it was not surprising that, for a fixed R , the NC values were higher in the anteroseptal than in the inferolateral myocardial regions. Indeed, the anteroseptal territories are less prone than the inferolateral to the auto attenuation of the body. This in turn imply that at a fixed R , the NC exhibited by the anteroseptal will be higher than the corresponding values in the posterolateral or, from a different perspective that higher R would be needed to reduce the NC values to the levels of the posterolateral regions.

The scanner/software combination resulted also to be a main effect with a significant impact (although with the lowest weight) on the NC. Again, the source of the difference was explained by the superior properties in terms of capability to recover the NC, particularly in the inferior regions, provided by solid-state gamma camera in comparison with Anger Cameras, while the differences in software between the conventional gamma cameras did not provide any significant difference between the two scanner/software combinations.

Both these last two findings were somewhat expected due to the different characteristics of the attenuation profile in different positions of the

myocardial wall and due to the superior characteristics in terms of contrast recovery provided by solid-state cameras.

The principle of optimization of patient's radiation exposure is defined and updated by the International Commission on Radiological Protection, ICRP²² and is best described as the management of radiation dose to the patient to be commensurate with the medical purpose. The optimization of protection in medical exposures does not necessarily mean the reduction of dose to the patient. However, in the present context, the demonstration that the activity ratio between rest and stress in the single-day stress-first MPI protocol which minimize cross talk between the stress and rest phase is 2:1 instead of being 3:1, which is the ratio currently adopted in the clinical practice, implies that this lower ratio should be used to fulfill the principle of optimization, since a higher ratio will not provide additional benefits while imparting a higher radiation dose to the patient.

LIMITATIONS OF THE STUDY

Some limitations of this study should be recognized. First, we assumed a 3-hour delay between the initial stress scan and the subsequent rest scan. The time to rest imaging after the stress dose varies considerably from 30-40 minutes¹ to several hours.¹⁵ Although a 3-hour delay would be preferable in order to decrease on-board stress activity and minimize the "ghosting" effect in subsequent resting scan, at least in the United States such a delay is seldom employed and current ASNC guidelines suggest a 2-hour delay with a 3:1 ratio of activities or no delay with a 3:5-4:1 ratio.⁴ It is likely that more studies or modeling are needed to clarify and codify these issues with modern SPECT cameras and software. However, we do not have conclusive data to ascertain if our results of no advantage with an $R > 2.0$ still hold in case of a reduced delay between stress and rest images.

Secondly, due to the lack of attenuation correction, the introduction of BC_{PD} in session 3 was needed to normalize the effect of attenuation. Session 3 data would not have been needed if attenuation correction was performed.

NEW KNOWLEDGE GAINED

Although current guidelines propose a rest-stress activity ratio of 3:1 in the one-day stress-first SPECT myocardial imaging, evidence is limited, and a lower ratio could be beneficial from the patient' radioprotection point of view. We demonstrated, in a phantom experiment using both CZT-based and conventional

gamma cameras and different reconstruction methods, that the optimal ^{99m}Tc activity ratio between rest and stress in the single-day stress-first MPI protocol to minimize cross talk between the stress and the rest phase is 2:1, significantly lower than generally employed.

CONCLUSIONS

The optimal ^{99m}Tc activity ratio between rest and stress in the single-day stress-first MPI protocol to minimize cross talk between the stress and the rest phase is 2:1, when a delay of 3 hours between the stress and the rest acquisition is adopted. Injecting the rest phase with the former recommended ratio of 3:1 is not to an optimized practice and will expose the patient to an increased and unnecessary level of radiation dose.

Acknowledgements

This study is dedicated to Professors Eugenio Inglese MD and Giovanni Lucignani MD who died during the COVID-19 pandemic. We are deeply grateful and honored to have worked with these enthusiastic teachers who trusted in the tight collaboration between nuclear medicine and medical physics.

Author Contributions

Study concept and design: O Zoccarato, M. Lecchi, R. Matheoud, C. Marcassa, M. Brambilla. Data acquisition: O Zoccarato, M. Lecchi, R. Matheoud, C. Scabbio. Analysis and interpretation of data: O Zoccarato, M. Lecchi, R. Matheoud, C. Marcassa, C. Scabbio, M. Brambilla. Drafting of the manuscript: O Zoccarato, M. Lecchi, R. Matheoud, C. Marcassa, C. Scabbio, M. Brambilla. Clinical revision of the manuscript for important intellectual content: O Zoccarato, M. Lecchi, R. Matheoud, C. Scabbio, C. Marcassa, M. Brambilla. Final approval of the manuscript submitted: all authors

Disclosure

No potential conflict of interest relevant to this article was reported.

References

1. DePuey EG, Ata P, Wray R, Friedman M. Very low-activity stress/high-activity rest, single-day myocardial perfusion SPECT with a conventional sodium iodide camera and wide beam reconstruction processing. *J Nucl Cardiol* 2012;19:931-44.
2. Nakajima K, Taki J, Shuke N, Bunko H, Takata S, Hisada K. Myocardial perfusion imaging and dynamic analysis with technetium-99m tetrofosmin. *J Nucl Med* 1993;34:1478-84.
3. Schulz G, Ostwald E, Kaiser HJ, vom Dahl J, Kleinhans E, Buell U. Cardiac stress-rest single-photon emission computed tomography with technetium 99m-labeled tetrofosmin: Influence of washout kinetics on regional myocardial uptake values of the rest study with a 1-day protocol. *J Nucl Cardiol* 1997;4:298-301.

4. Henzlva MJ, Duvall WL, Einstein AJ, Travin MI, Verberne HJ. ASNC imaging guidelines for SPECT nuclear cardiology procedures: Stress, protocols, and tracers. *J Nucl Cardiol* 2016;23:606-39.
5. Hesse B, Tägil K, Cuocolo A, Anagnostopoulos C, Bardiés M, Bax J, et al. EANM/ESC procedural guidelines for myocardial perfusion imaging in nuclear cardiology. *Eur J Nucl Med Mol Imaging* 2005;32:855-97.
6. Garcia EV, Cooke CD, Van Train KF, Folks R, Peifer J, DePuey EG, et al. Technical aspects of myocardial SPECT imaging with technetium-99m sestamibi. *Am J Cardiol* 1990;66:23E-31E.
7. Verberne HJ, Acampa W, Anagnostopoulos C, Ballinger J, Bengel F, De Bondt P, et al. EANM procedural guidelines for radionuclide myocardial perfusion imaging with SPECT and SPECT/CT: 2015 revision. *Eur J Nucl Med Mol Imaging* 2015;42:1929-40.
8. Hyafil F, Gimelli A, Slart R.H.J.A., Georgoulas P, Rischpler C, Lubberink M et al. EANM procedural guidelines for myocardial perfusion scintigraphy using cardiac-centered gamma cameras. *European J Hybrid Imaging* 2019;3:11. <https://doi.org/10.1186/s41824-019-0058-2>
9. Zoccarato O, Scabbio C, De Ponti E, Matheoud R, Leva L, Morzenti S et al. Comparative analysis of iterative reconstruction algorithms with resolution recovery for cardiac SPECT studies. A multi-center phantom study. *J Nucl Cardiol* 2014;21:135-48.
10. Zoccarato O, Lizio D, Savi A, Indovina L, Scabbio C, Leva L, et al. Comparative analysis of cadmium-zinc-telluride cameras dedicated to myocardial perfusion SPECT: A phantom study. *J Nucl Cardiol* 2016;23:885-93.
11. Zoccarato O, Marcassa C, Lizio D, Leva L, Lucignani G, Savi A, et al. Differences in polar-map patterns using the novel technologies for myocardial perfusion imaging. *J Nucl Cardiol* 2017;24:142-4.
12. Munch G, Nerverve J, Matsunari I, Schroter G, Schwaiger M. Myocardial technetium-99m-tetrofosmin and technetium-99m-sestamibi kinetics in normal subjects and patients with coronary artery disease. *J Nucl Med* 1997;38:428-32.
13. van Dijk JD, van Dalen JA, Knollema S, Mouden M, Ottervanger JP, Jager PL. Minimal rest activity for SPECT myocardial perfusion imaging in a one-day stress-first protocol. *Eur J Nucl Med Mol Imaging* 2019;46:1248-56.
14. Kirac S, Franc J Th W, Liu Y. Validation of the Yale circumferential quantification method using (201)Tl and (99m)tc: A phantom study. *J Nucl Med* 2000;41:1436-41
15. Sharir T, Pinskiy M, Pardes A, et al. Comparison of the diagnostic accuracies of very low stress-dose with standard-dose myocardial perfusion imaging: Automated quantification of one-day, stress-first SPECT using a CZT camera. *J Nucl Cardiol* 2016;23:11-20.
16. Palyo RJ, Sinusas AJ, Liu YH. High-sensitivity and high-resolution SPECT/CT systems provide substantial dose reduction without compromising quantitative precision for assessment of myocardial perfusion and function. *J Nucl Med* 2016;57:893-9.
17. Einstein AJ, Johnson LL, DeLuca AJ, et al. Radiation dose and prognosis of ultra-low-dose stress-first myocardial perfusion SPECT in patients with chest pain using a high-efficiency camera. *J Nucl Med* 2015;56:545-51.
18. Chang SM, Nabi F, Xu J, Raza U, Mahmarian JJ. Normal stress-only versus standard stress/rest myocardial perfusion imaging: Similar patient mortality with reduced radiation exposure. *J Am Coll Cardiol* 2010;55:221-30.
19. Duvall WL, Guma KA, Kamen J, Croft LB, Parides M, George T, Henzlva MJ. Reduction in occupational and patient radiation exposure from myocardial perfusion imaging: Impact of stress-only imaging and high-efficiency SPECT camera technology. *J Nucl Med* 2013;54:1251-7.

20. Mercuri M, Pascual TN, Mahmarian JJ, Shaw LJ, Dondi M, Paez D, et al. Estimating the reduction in the radiation burden from nuclear cardiology through use of stressonly imaging in the united states and worldwide. *JAMA Intern Med* 2016;176:269-73.
21. Lecchi M, Malaspina S, Scabbio C, Gaudieri V, Del Sole A. Myocardial perfusion scintigraphy dosimetry: Optimal use of SPECT and SPECT/CT technologies in stress-first imaging protocol. *Clin Transl Imaging* 2016;4:491-8.
22. International Commission on Radiological Protection The 2007 Recommendations of the International Commission on Radiological Protection. ICRP Publication 103 Ann ICRP 2007;37:1-332.

Publisher's Note Springer Nature remains neutral with regard to jurisdictional claims in published maps and institutional affiliations.